A SECOND-ORDER PDE TECHNIQUE TO CONSTRUCT DISTANCE FUNCTIONS WITH MORE ACCURATE DERIVATIVES.

Siddharth Manay *Anthony Yezzi*

School of Electrical and Computer Engineering
Georgia Institute of Technology
Atlanta, GA 30332
{smanay.ece98@gtalumni.org ayezzi@ece.gatech.edu}

ABSTRACT

In this paper we demonstrate the use of an anisotropic PDE to improve the behavior of first and second derivatives of a distance function. We begin by deriving a property of these derivatives and showing a natural relationship between this property and the *anti-geometric heat flow*. We then construct a PDE that combines a known first-order PDE with the anti-geometric flow and then demonstrate its effectiveness with a discrete simulation.

1. INTRODUCTION

A distance function is a mapping that describes the distance from a point to a given set, usually a surface embedded in R^n. In many applications, the surface is known and does not change, so the distance function can be computed *a priori*. Applications that rely such mappings include image registration and curve matching. If image registration is approached as an optimization problem to be solved using gradient descent methods, as in [1], then the distance function needs to be differentiable. For a higher order method such as quasi-Newton optimization, second derivatives are also required.

There are many algorithms to compute discrete approximations of a distance function, ranging from chamfer algorithms [2] to PDE-based frameworks and fastmarching algorithms. These range in accuracy and differentiability. Even for accurate algorithms, such as the fastmarching algorithm [3], the accuracy of the function and its derivatives is limited by the accuracy of the representation of the surface. In this case, the distance values adjacent to the surface (represented as a level set) are initialized very coarsely; the first and second derivatives cannot be expected to be accurate, especially in this region.

We present a PDE designed to improve the properties of the first and second derivatives of distance functions by exploiting the natural connection between the properties of a distance function and an anisotropic heat flow, specifically the anti-geometric flow. Based on this connection, we construct a PDE which integrates a first-order PDE (derived from the Eikonal equation) with the anti-geometric flow. We demonstrate that this combined PDE will improve the behavior of the first and second derivatives.

The remainder of this paper is structured as follows. In Section 2 we derive a property of the second derivatives of a distance function. We then discuss the anti-geometric heat flow in Section 3 and show the flow's relationship to distance functions. We validate this relationship with experimental results in Section 4 before concluding the discussion in Section 5.

2. CONDITION ON SECOND DERIVATIVES OF DISTANCE FUNCTIONS

In this section we derive a condition on the second derivatives of a distance function.

Distance functions are best characterized as satisfying the Eikonal equation,

$$\|\nabla\Phi\| = 1.$$

This equation not only is the source of algorithms used to construct discrete approximations of these functions, but also provides a condition on the first derivatives. In [4], the authors construct a PDE that can be used to improve the properties the first derivatives of approximate distance functions,

$$\frac{\partial\Phi}{\partial t} = \text{sgn}(\Phi)(1 - \|\nabla\Phi\|). \tag{1}$$

This first-order PDE does not guarantee the accuracy of the second derivatives, however.

A condition on the second derivatives of Φ can be constructed by restating the Eikonal equation as

$$\nabla\Phi^T \cdot \nabla\Phi = 1$$

and taking ∇ of both sides, yielding

$$\nabla^2\Phi\nabla\Phi = \vec{0}. \tag{2}$$

where $\nabla^2\Phi$ denotes the Hessian of Φ.

3. ANTI-GEOMETRIC HEAT FLOW

In this section we first discuss the anti-geometric heat flow as it relates to image smoothing operators before showing its relationship to the second-order derivative properties of distance functions.

Typically, edge directions in an image are related to the tangents of the iso-intensity contours (level curves or level sets) of an image I. Let η denote the direction normal to the level curve through a given point (the gradient direction), and let ξ denote the tangent direction (see Figure 1). We may write these directions in terms of the first derivatives of the image I_x and I_y as

$$\eta = \frac{(I_x, I_y)}{\sqrt{{I_x}^2 + {I_y}^2}}, \quad \xi = \frac{(-I_y, I_x)}{\sqrt{{I_x}^2 + {I_y}^2}}.$$

Since η and ξ constitute orthogonal directions, we may express the rotationally invariant Laplacian operator (the kernel of

0-7803-7750-8/03/$17.00 ©2003 IEEE

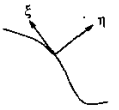

Fig. 1. Normal and tangent directions to a level curve.

the linear heat equation) as the sum of the second order spatial derivatives $I_{\eta\eta}$ and $I_{\xi\xi}$ in these directions and write the linear heat equation as

$$\frac{\partial I}{\partial t} = \nabla \cdot (\nabla I) = I_{\xi\xi} + I_{\eta\eta}.$$

This decomposition of the linear heat equation has been considered in many earlier works on anisotropic diffusion (see [5, 6, 7, 8, 9, 10] for a few examples).

Omitting the normal diffusion while keeping the tangential diffusion yields the well known *geometric heat flow*, which diffuses along the boundaries of image features but not across them. It derives its name from the fact that, under this flow, the level curves of the image evolve in the normal direction in proportion to their curvature. This model is well known for its ability to denoise images while maintaining sharp edges and is therefore widely used for image enhancement and smoothing. For more extensive discussions of the many properties of this flow and related flows see [11, 5, 9, 12, 13, 14, 15].

In [16] we discuss the applications of the flow constructed by omitting the tangential diffusion and keeping the normal diffusion. The general form for this compliment flow, which we refer to as the *anti-geometric heat flow*, is

$$I_{\eta\eta} = \frac{(\nabla I)^T \nabla^2 I (\nabla I)}{\|\nabla I\|^2}. \tag{3}$$

In the case of a distance function Φ, the derivative in the gradient direction $\Phi_\eta = 1$, which means

$$\Phi_{\eta\eta} = 0,$$

that is, distance functions are solutions to the anti-geometric PDE. We also note that the numerator of Equation 3 includes the term $\nabla^2 I \nabla I$, which is identical to the left-hand-side of Equation 2. This implies that, for a distance function, $\nabla\Phi^2\nabla\Phi$ and therefore the numerator of the anti-geometric PDE is zero, that is, at steady state. This is exactly the property we desire for the second derivatives of a distance function.

To ensure the stability of the zero-level set of the function and to improve the accuracy of the first derivatives along with the second derivatives, we combine the first-order PDE from Equation 1 with the anti-geometric heat flow, as follows.

$$\frac{\partial \Phi}{\partial t} = \mathrm{sgn}(\Phi)(1 - \|\nabla\Phi\|) + \Phi_{\eta\eta} \tag{4}$$

The observation that a distance function will satisfy this equation demonstrates the existence of a solution. The unicity of the solution is discussed in Section 5.

4. EXPERIMENTAL RESULTS

In this section we discuss in the implementation of the PDE in Equation 4. We then introduce measures of the "fit" of the properties of the derivatives and compare the results of the PDEs using these metrics.

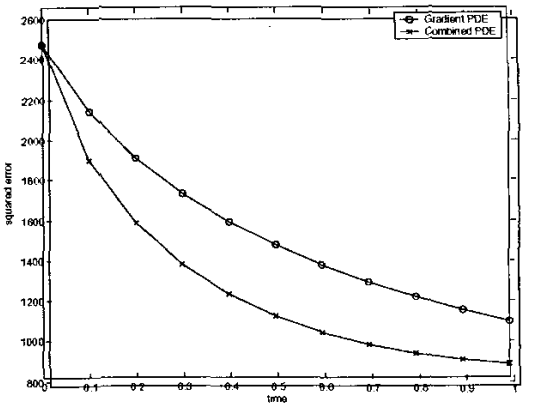

Fig. 2. Squared error versus time for two PDEs run on a synthetic distance function.

Discrete implementation of the first-order PDE must propagate information only in the upwind direction, as in the fastmarching algorithm. Specifically, we calculate $\|\nabla\Phi\|$ as in [17],

$$\begin{aligned}\|\nabla\Phi\| &= max(\Phi^{-x}, 0)^2 + min(\Phi^{+x}, 0)^2 \\ &+ max(\Phi^{-y}, 0)^2 + min(\Phi^{+y}, 0)^2 \\ &+ max(\Phi^{-z}, 0)^2 + min(\Phi^{+z}, 0)^2,\end{aligned}$$

where Φ^{-x} and Φ^{+x} represent the one-sided derivatives in the negative and positive x directions, respectively. Calculation of $\Phi_{\eta\eta}$ is simpler, as it relies only on central differences. The evolution is simulated using the Euler step method, with an approximate distance function (such as one constructed using the fastmarching algorithm) as a starting point.

We are foremost interested in the accuracy of any distance function. For examples where we can calculate the exact distance function Φ_0 analytically, the squared error of an approximation of Φ_0 is

$$E(\Phi) = \int_\Omega (\Phi - \Phi_0)^2 \, dv,$$

where Ω is the domain of the function. We further wish to measure the properties of the first and second derivatives. As stated before, the distance function satisfies the Eikonal equation everywhere, except at shocks. To measure how well an approximate distance function obeys this property, we introduce a measure on the gradient of the function,

$$M_1(\Phi) = \int_\Omega |1 - \|\nabla\Phi\|| \, dv.$$

Similarly, we construct a measure on the Hessian of the distance function to measure the deviation from the second derivative property in Equation 2,

$$M_2(\Phi) = \int_\Omega \|\nabla^2\Phi\nabla\Phi\| \, dv.$$

In Figures 2, 3 and 4 we show experimental values for the error, gradient measure, and Hessian measure of the distance function as a function of the time the PDE is run. In this experiment, we restrict Ω to a small neighborhood around the zero level curve,

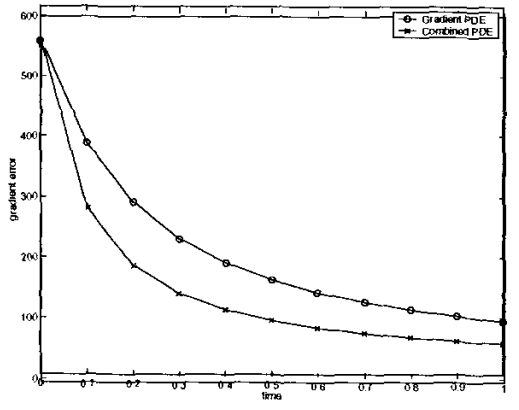

Fig. 3. Gradient error versus time for two PDEs run on a synthetic distance function.

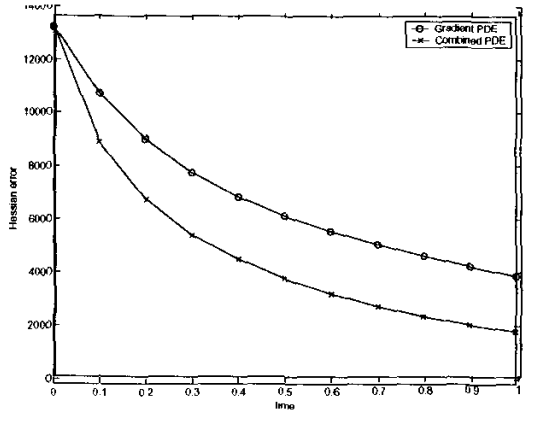

Fig. 4. Hessian error versus time for two PDEs run on a synthetic distance function.

($\Omega = \{x|\Phi(x) < 2\}$) to emphasize the improvement for the initial values of the fastmarching algorithm. The distance function, in this case the distance from a symmetric cluster of six spheres, was initialized using the fastmarching algorithm. In both figures, we compare the first-order PDE and the PDE combining the first-order and anti-geometric terms (as in Equation 4). We begin with Figure 2, showing that, for short runs, the PDE that includes the anti-geometric flow improves the overall error of the distance function. Figure 3 demonstrates that anti-geometric term, when used in conjunction with the first-order PDE, reduces the norm of the gradient more than just the first-order PDE alone. Figure 4, shows the affect of the two PDEs on the second-order property. Including the anti-geometric term reduces $M_2(\Phi)$ more than 50% (at $t = 1$) compared to the first-order PDE alone.

The graphs in Figures 6 and 7 show the effect of the application of the combined PDE to a distance function around the a surface segmented from a MRI. A cross-section of the skin surface segmentation and the distance function constructed around this surface are shown in Figure 5. Again, for this experiment Ω is

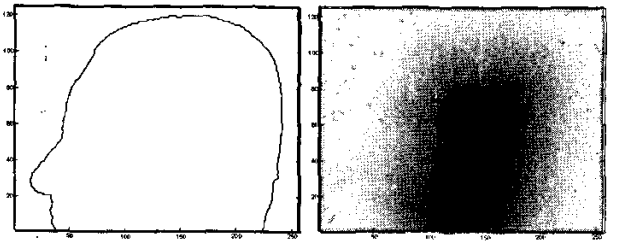

Fig. 5. Cross sections of skin surface segmentation [left] and signed distance function [right].

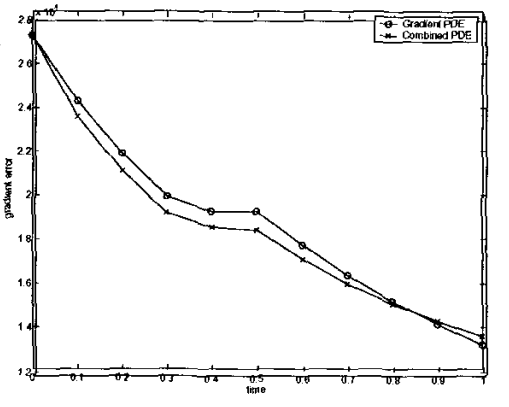

Fig. 6. Gradient metric versus time for two PDEs run on the skin surface distance function.

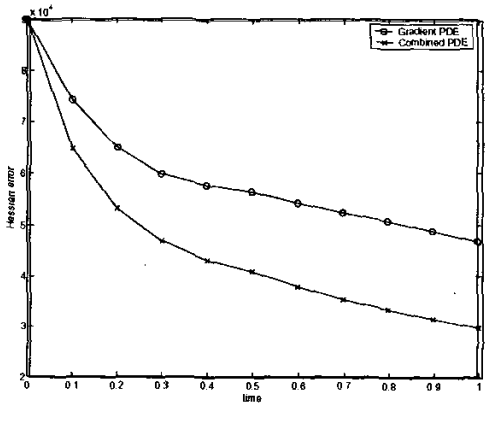

Fig. 7. Hessian metric versus time for two PDEs run on a skin surface distance function.

limited to a small neighborhood around the zero level curve. We are unable to demonstrate the effects on squared error, since there is no analytic "ground truth" for this example. However, Figure 6 demonstrates that, for short runs of the PDE, the combined flow subtly improves the first-order properties of the distance functions. The more obvious benefit can be seen in Figure 7, a graph of the second-order properties of the function, where the combined PDE again reduces the Hessian measure.

5. CONCLUSION

In the previous section, we improved the first- and second-order properties of distance functions using short runs of the combined PDE. Before concluding, we note some properties of the anti-geometric term that make long runs this PDE ill-suited for the numerical calculation of distance functions.

In general the evolution of the combined PDE *diverges* from a distance function, even when initialized with an approximate distance function. Stated another way, although distance functions satisfy the anti-geometric PDE, they are not stable solutions to this PDE. (Stable solutions include functions I with the property I_x and I_y are constant everywhere.) Intuition affirming this observation begins by recalling that the anti-geometric flow reduces the magnitude of the norm of the gradient. Numerical approximations of the distance function, like the fastmarching algorithm, do not guarantee that $\|\nabla\Phi\| = 1$ everywhere. In regions where $\|\nabla\Phi\| < 1$ due to numerical errors or shocks, the anti-geometric flow will always further reduce the norm, diverging from the desired distance function. We combine the anti-geometric term with the first-order term in Equation 1, which drives the gradient to 1, to combat this effect; but we cannot guarantee that the steady state of Equation 4 is a distance function.

Another explanation begins by recalling that anti-geometric flow obeys the maximum principle. This means that the evolution of the PDE is always bounded above and below by the initial condition, that is, the function is everywhere greater than the minimum value of the initial function and less than the maximum value. In the case of distance functions, the anti-geometric PDE can drive the initial function toward the true distance function only if the initial function bounds the distance function. In general, schemes for generating approximate distance functions do not guarantee this.

In this paper, we have discussed the application of an anisotropic PDE to improve the behavior of first and second derivatives of an approximate distance function. We first derived a simple condition on the second derivatives, and then demonstrated a link between this condition and anti-geometric heat flow. We then validated this result via simulation, demonstrating that an anti-geometric term, coupled with a first-order PDE, effectively reduces the error in the desired properties of the first and second derivatives of a distance function.

6. REFERENCES

[1] O. Cuisenaire, *Distance Transformations: Fast Algorithms and Applications to Medical Image Processing*, Ph.D. thesis, Laboratoire de Telecommunications et Teledetection, 1999.

[2] G. Borgefors, "Hierarchical camfer matching: A parametric edge matching algorithm," *IEEE Trans. on Pat. Anal. and Mach. Intel.*, vol. 10, no. 6, Nov 1988.

[3] J. Sethian, "A fast marching level set method for monotonically advancing fronts," *Proceedings. Natl. Acad. Sci. USA*, vol. 93, pp. 1591–1595, Feb 1996.

[4] M. Sussman, P. Smereka, and S. J. Osher, "A level set method for computing solutions to incompressible two-phase flow," *J. Comp. Phys.*, vol. 114, pp. 146–159, 1994.

[5] L. Alvarez, P. L. Lions, and J. M. Morel, "Image selective smoothing and edge detection by nonlinear diffusion. II," *SIAM J. Numer. Anal.*, vol. 29, pp. 845–866, 1992.

[6] R. Carmona and S. Zhong, "Adaptive smoothing respecting feature directions," *IEEE Trans. on Image Proc.*, vol. 7, no. 3, pp. 353–358, 1998.

[7] G. Unal, H. Krim, and A. Yezzi, "Feature-preserving flows: A stochastic differential equations's view," vol. 1, pp. 896–899, Sep 2000.

[8] R. Whitaker and S. Pizer, "A multi-scale approach to nonuniform diffusion," *Comp. Vision, Graphics, and Image Proc. – Image Understanding*, vol. 57, no. 1, pp. 99–110, Jan 1993.

[9] B. B. Kimia and K. Siddiqi, "Geometric heat equation and nonlinear diffusion of shapes and images," *Proceedings of Comp. Vis. and Pat. Rec.*, 1994.

[10] Y. L. You, W. Xu, A. Tannenbaum, and M.Kaveh, "Behavioral analysis of anisotropic diffusion in image processing," *IEEE Trans. on Image Proc.*, vol. 5, pp. 1539–1553, 1996.

[11] L. Alvarez, F. Guichard, P. L. Lions, and J. M. Morel, "Axioms and fundamental equations of image processing," *Archives Rational Mech. Anal.*, vol. 123, 1993.

[12] B. B. Kimia, A. Tannenbaum, and S. W. Zucker, "On the evolution of curves via a function of curvature, I the classical case," *J. Math., Anal., and App.*, vol. 163, pp. 438–458, 1992.

[13] R. Malladi and J.Sethian, "A unified approach to noise removal, image enhancement, and shape recovery," *IEEE Trans. on Pat. Anal. and Mach. Intel.*, vol. 5, pp. 1554–1568, 1996.

[14] G. Sapiro and A. Tannenbaum, "On invariant curve evolution and image analysis," *Indiana Univ. J. of Math.*, vol. 42, 1993.

[15] G. Sapiro and A. Tannenbaum, "Affine invariant scale-space," *Int'l J. Comp. Vision*, vol. 11, pp. 25–44, 1993.

[16] S. Manay and A. Yezzi, "Anti-geometric diffusion for adaptive thresholding and fast segmentation," *IEEE Trans. on Image Proc.*, Jul 2001, To appear.

[17] J. Sethian, *Level Set Methods and Fast Marching Methods*, Cambridge University Press, Cambridge, UK, 1999.